



# Monitoring Shallow Infiltration in Sandy Soil using GPR Groundwave Techniques

Michael Kristoff, Audrey Mohr, Anya Benda, Taylor Crist and Dr. Katherine Grote  
Department of Geology - University of Wisconsin Eau Claire



## INTRODUCTION

Characterizing the near-surface soil water content distribution is important for precision agriculture and groundwater remediation applications. Measuring soil water content over large areas is often difficult, as conventional point measurement and remote sensing techniques are often insufficient to characterize water content heterogeneity at the field scale. Ground penetrating radar (GPR) groundwaves are an electromagnetic geophysical technique that can be used to estimate water content quickly over large areas, and recent studies have indicated that the groundwave sampling depth is a function of antenna frequency (Grote et al., 2010). The objective of this field-scale research is to explore the potential of multi-frequency GPR groundwave data for detecting changes in soil moisture at different depths as water moves through the near-surface soil.

## BACKGROUND

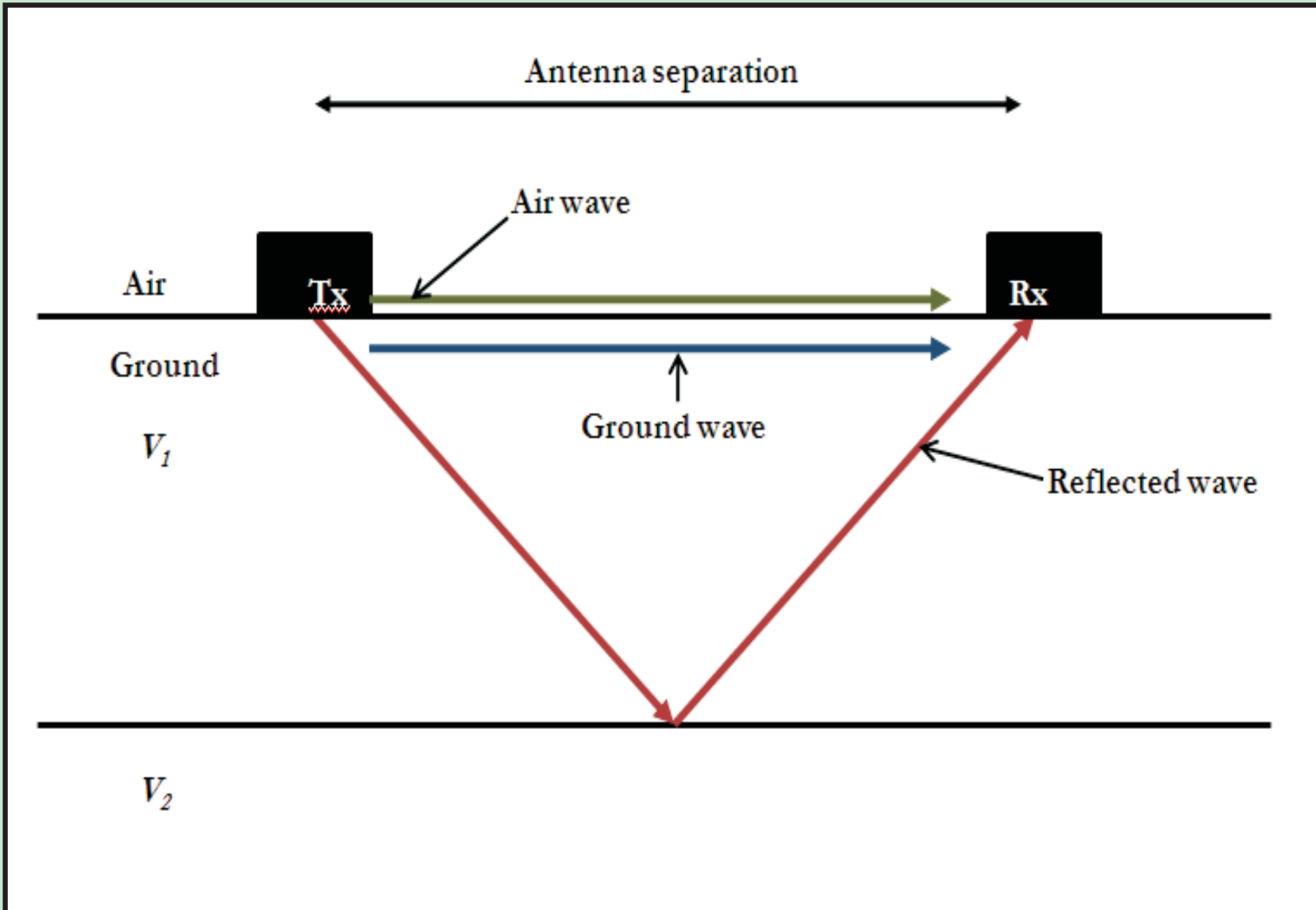


Figure 1: GPR groundwaves travel in the shallow subsurface directly between the GPR transmitter (TX) and receiver (RX).

GPR groundwaves are direct waves that travel in the shallow subsurface between the transmitting and receiving antennas (Figure 1). Groundwaves travel at the electromagnetic velocity of the near-surface soil, so the soil velocity can be estimated by measuring the time needed for the groundwave to travel from the transmitting antenna to the receiving antenna and the distance between these antennas. The electromagnetic velocity is primarily dependent upon the soil water content, so after the velocity is estimated, it can be converted to volumetric water content (VWC) using a petrophysical relationship.

## DATA ACQUISITION

GPR groundwave data were acquired in six rows over a gently sloping, 11-acre field site of predominantly coarse-grained soil in northern Wisconsin (Figure 2). GPR data were obtained using three antenna pairs with central frequencies of 100-, 500-, and 1000-MHz. Variable-offset surveys were acquired to determine an appropriate antenna separation for common-offset data and to aid with data interpretation. Common-offset data were then acquired using a sled system and a multi-channel adapter that allowed simultaneous data acquisition with multiple antenna pairs (Figure 3). Data were acquired before irrigation began, soon after irrigation ended, and 7 hours after irrigation ended.

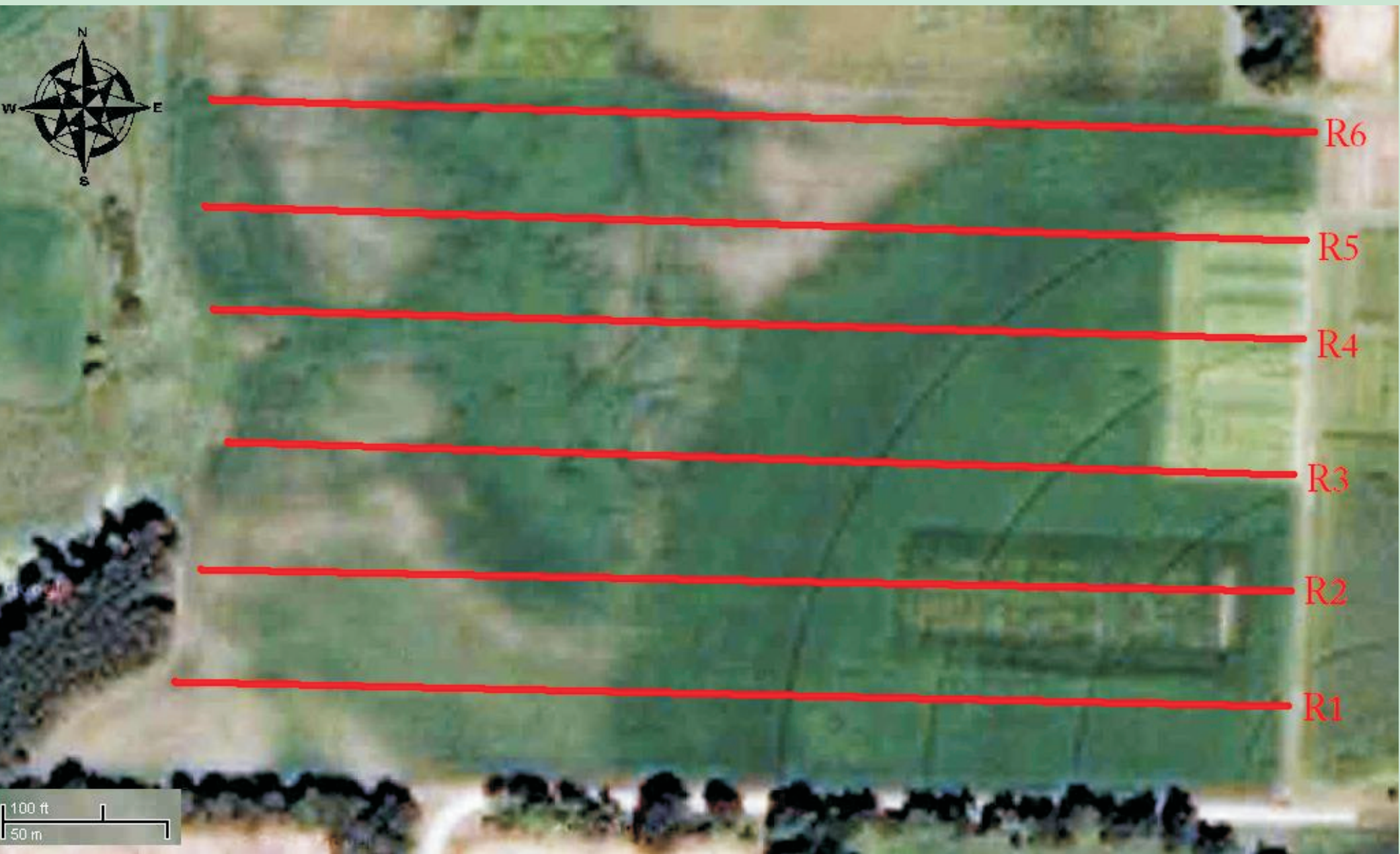


Figure 2: GPR data were acquired in six traverses across the site.



Figure 3: GPR data were acquired simultaneously for all frequencies using a sled system.

## DATA ANALYSIS

For each GPR frequency, variable-offset GPR surveys were used to identify the airwave and groundwave based upon their arrival times and velocities (Figure 4). Then, the arrival time of the airwave and groundwave at the antenna separation used in the common-offset data acquisition was noted. These arrival times (and the wavelet pattern observed in the variable-offset data) were used to identify the airwave and groundwave wavelets in the common-offset data. The arrival times for both the airwave and groundwave in the common-offset data were noted for each measurement (Figure 5), and these times were used to calculate the time needed for the groundwave to travel between antennas. The groundwave travel time was then used to calculate the groundwave velocity. Topp's equation (Topp et al., 1980) was used to convert the velocity measurements to VWC estimates.

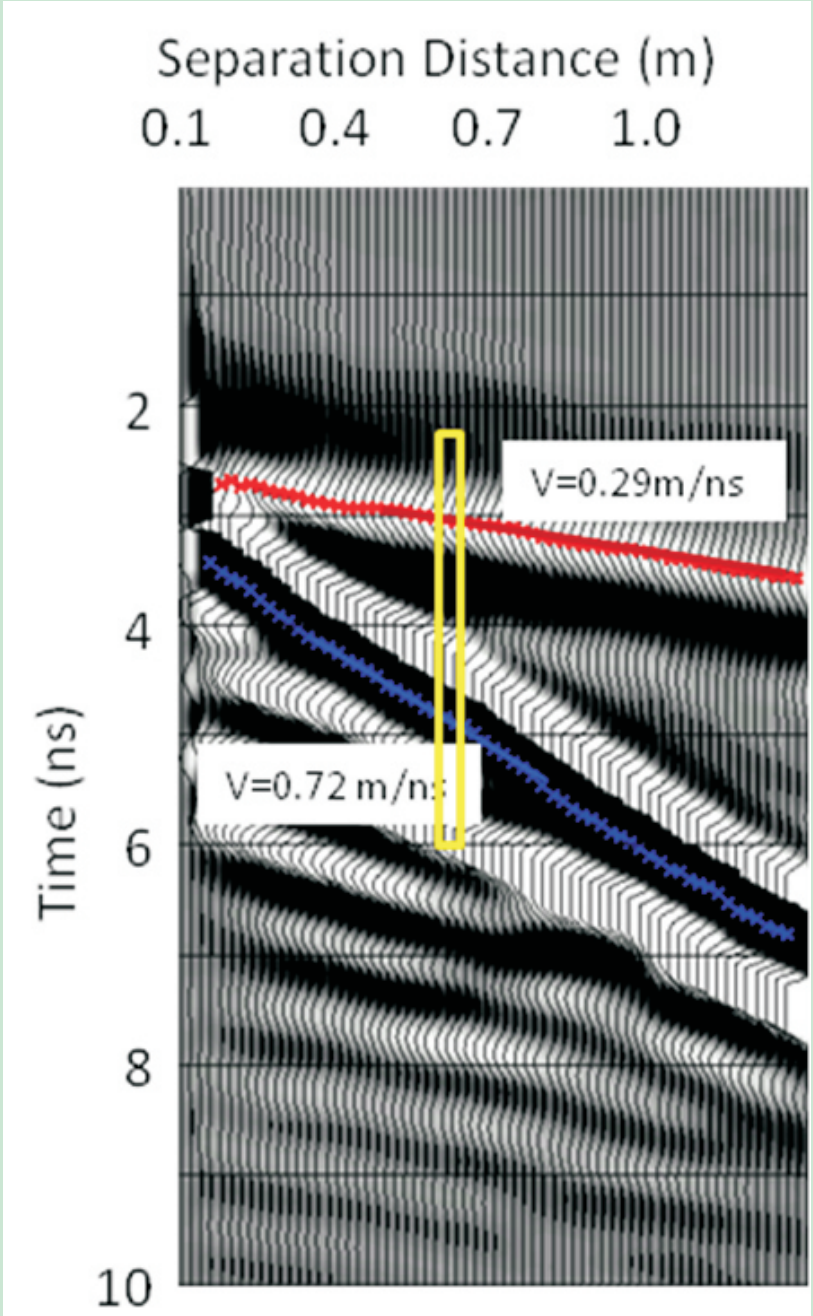


Figure 4: Variable offset data acquired with 500 MHz antennas. The box shows the separation distance between antennas at which the common-offset data were acquired.

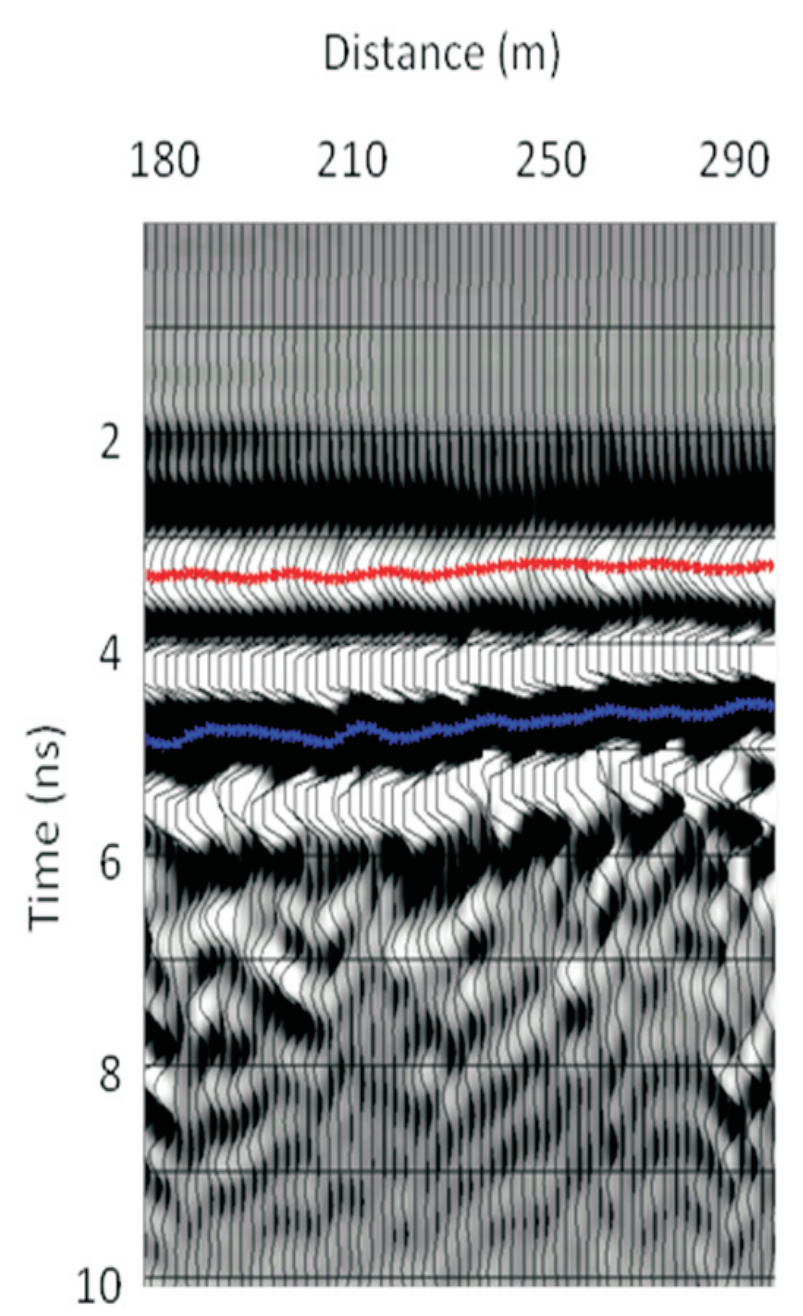


Figure 5: Common-offset 500 MHz data acquired along Row 1. Variations in the groundwave travel time indicate changes in soil moisture.

## RESULTS

Table 1 and Figures 6, 7, and 8 show the VWC estimated from GPR data acquired before, soon after, and 7 hours after infiltration for each frequency, as well as the approximate sampling depth for each frequency. These results show that all frequencies detected increased water content after irrigation, but not at the same times. The shallow 1000 MHz data showed a significant increase in water content in the morning, immediately after irrigation. At ~7 hours after irrigation, the shallowest soil had dried somewhat, although the average water content was still greater than its pre-irrigation value. In the slightly deeper 500 MHz data, a similar pattern was observed, with a large initial increase in moisture, followed by slight drying. These results indicate that water seeped into the shallow soil fairly quickly, but some of the moisture was later lost due to evapotranspiration or to continued infiltration into deeper layers. In the deeper 100 MHz data, a slight increase in water content was observed immediately after infiltration, with a more significant increase occurring several hours later. This pattern indicates that the 100 MHz antennas were somewhat influenced by the very shallow increase in moisture immediately after irrigation, but the increase in soil moisture over a larger vertical interval (as the infiltration front moved deeper into the soil profile) caused a greater response in the GPR measurements. Thus, water can be seen to be moving out of the shallower soil (measured by 1000 and 500 MHz data) and into deeper soil layers by ~7 hours after irrigation.

Frequency (MHz)	1000	500	100
Predicted sampling depth (in)	2.7	4.4	8.3
Average VWC across field before irrigation	0.28	0.16	0.20
Average VWC across field immediately after irrigation	0.36	0.20	0.21
Average VWC across field 7 hours after irrigation	0.31	0.19	0.24

Table 1: Average volumetric water content (VWC) over irrigated area at different times.

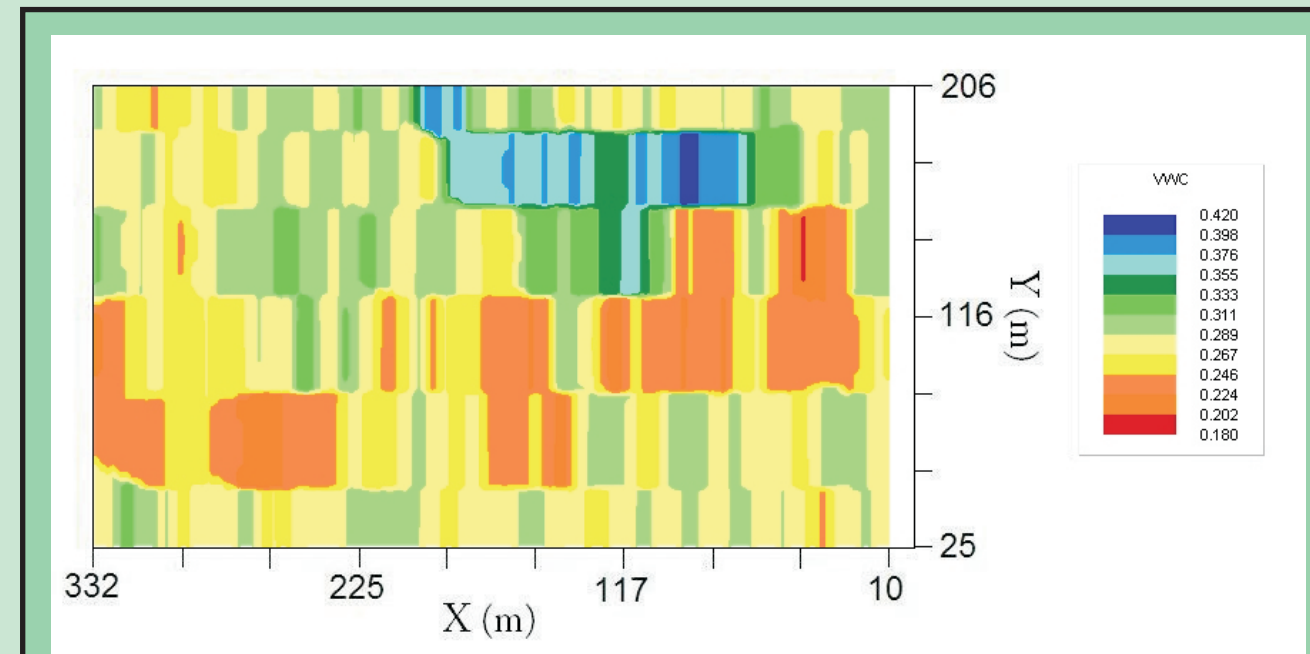


Figure 6a: 1000 MHz data acquired before irrigation.

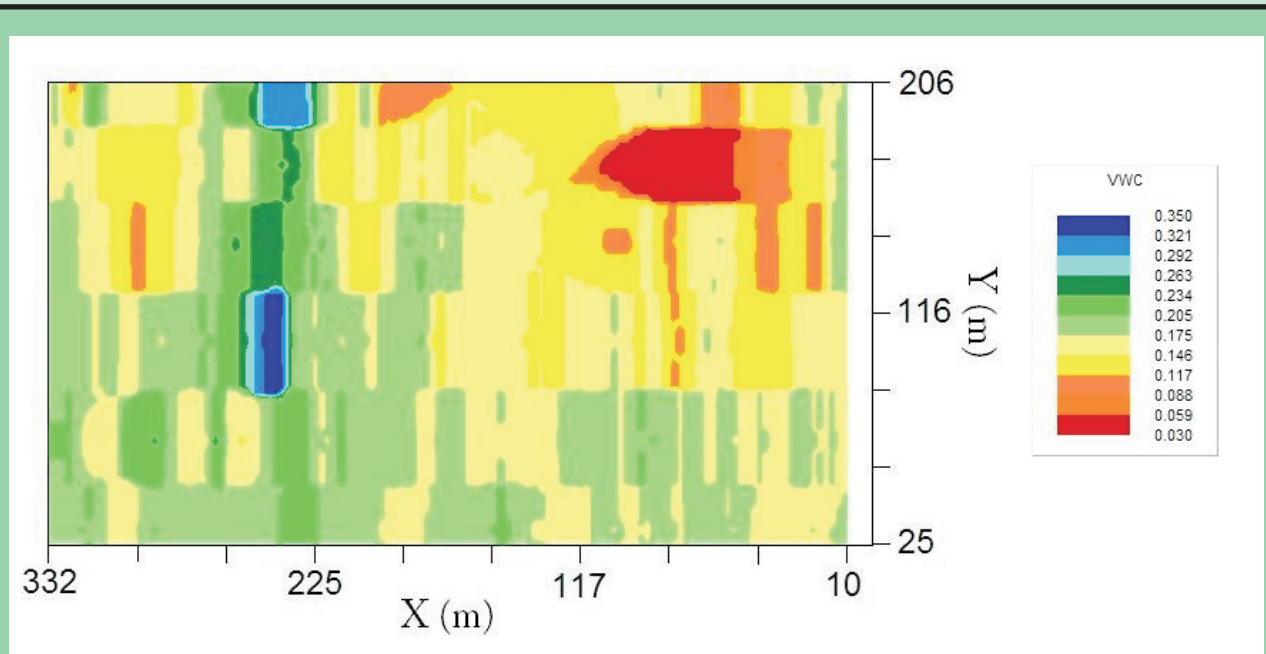


Figure 7a: 500 MHz data acquired before irrigation.

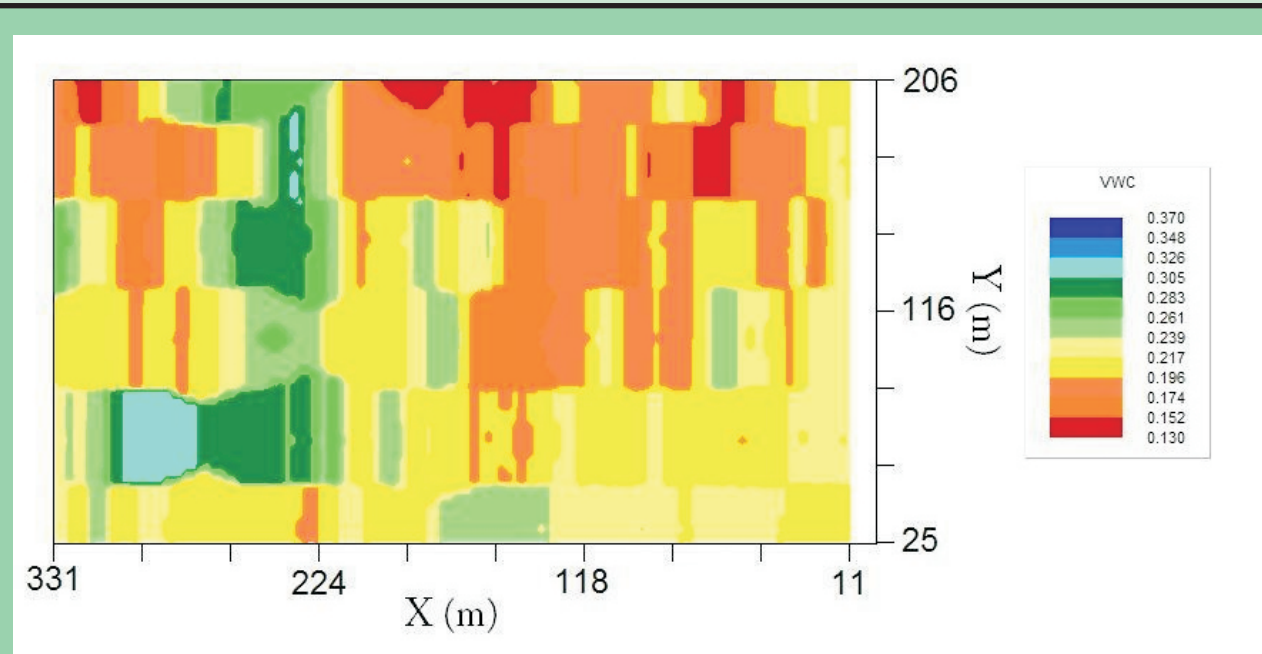


Figure 8a: 100 MHz data acquired before irrigation.

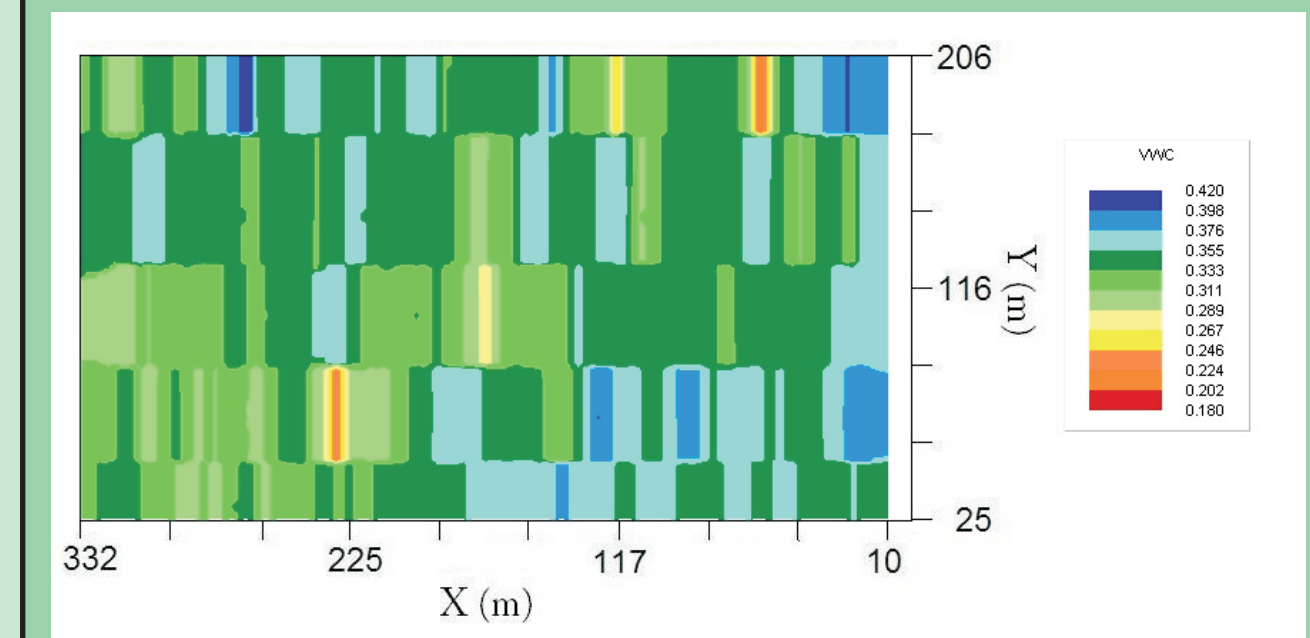


Figure 6b: 1000 MHz data acquired immediately after irrigation.

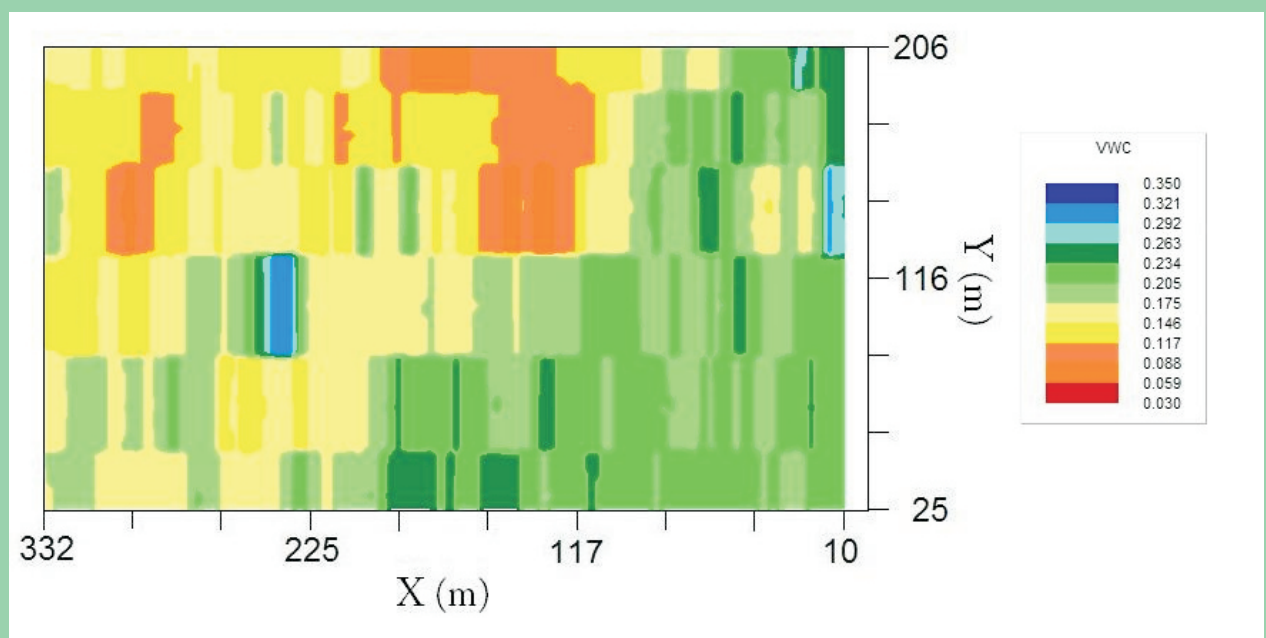


Figure 7b: 500 MHz data acquired immediately after irrigation.

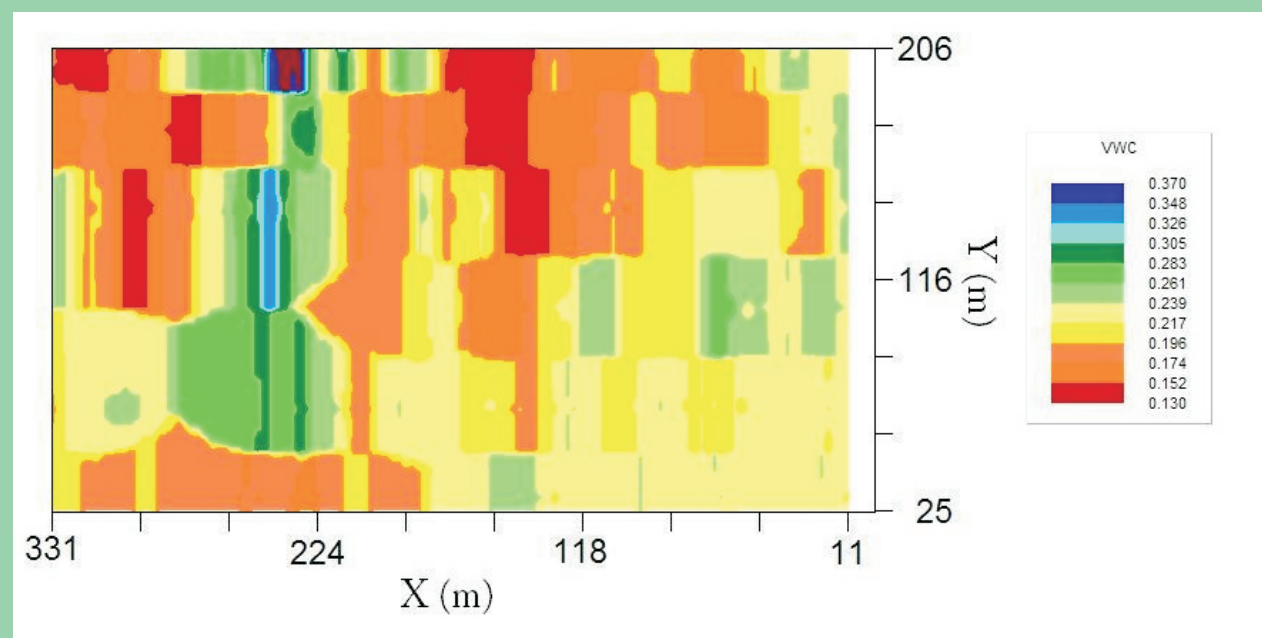


Figure 8b: 100 MHz data acquired immediately after irrigation.

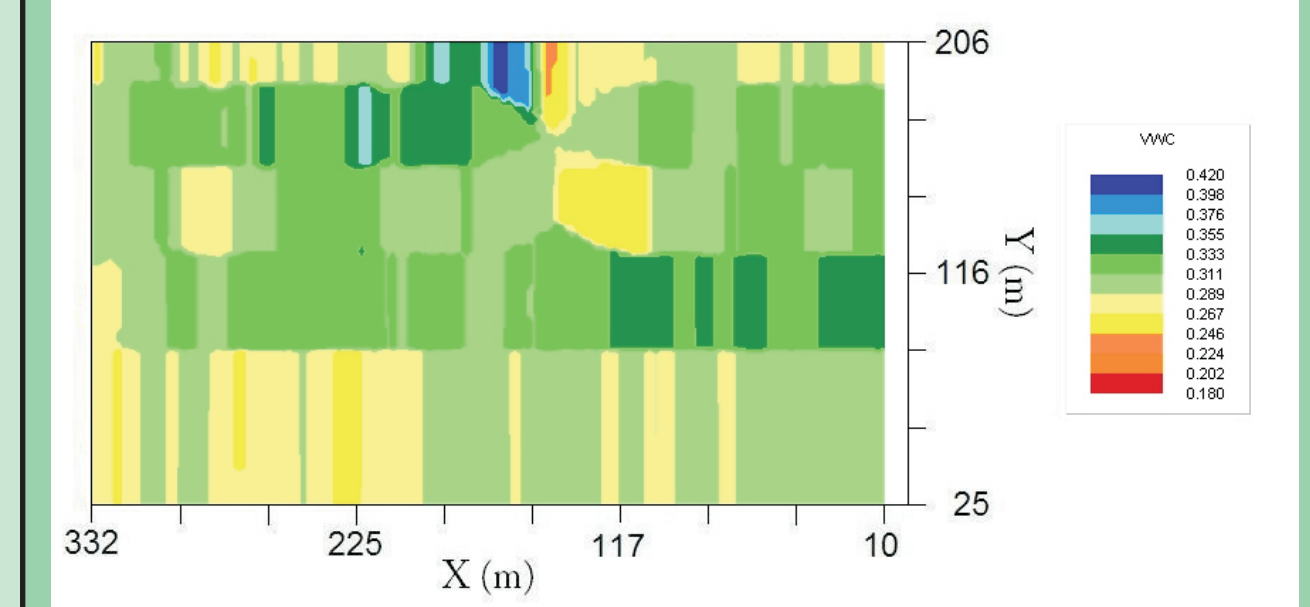


Figure 6c: 1000 MHz data acquired 7 hours after irrigation.

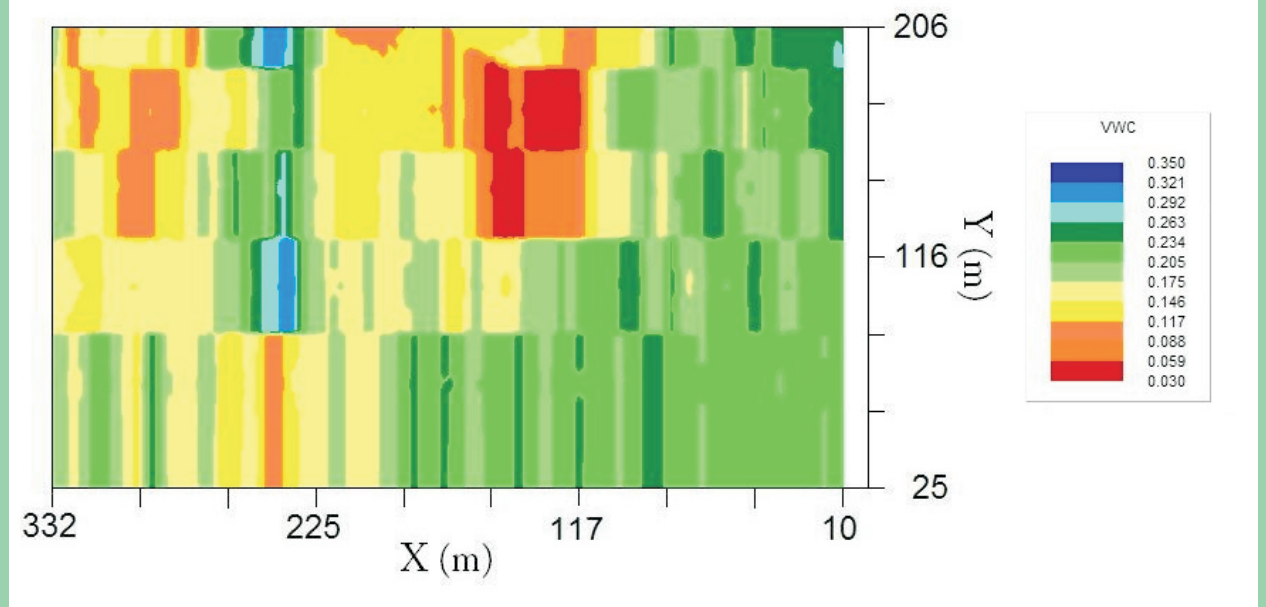


Figure 7c: 500 MHz data acquired 7 hours after irrigation.

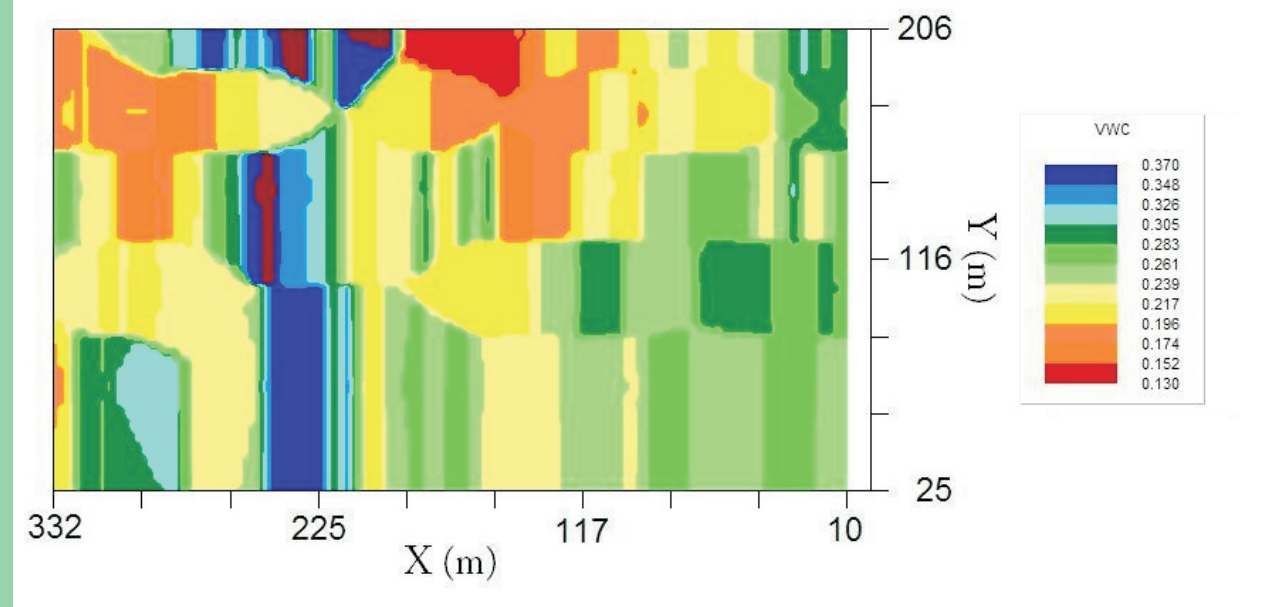


Figure 8c: 100 MHz data acquired 7 hours after irrigation.

## CONCLUSIONS

The results from this experiment show that multi-frequency GPR groundwave data can be used to monitor infiltration as it moves through a soil column. The higher frequencies (shallower sampling depths) showed the most variation in water content and showed wetting immediately after irrigation, followed by drying several hours later, while the deeper GPR measurements (lower frequencies) showed a greater increase in water content at longer times after irrigation. When the GPR groundwave sampling depth sensitivity has been more fully defined, GPR groundwave measurements could be used to more accurately map the progress of an infiltration front and might be used to estimate parameters such as the hydraulic conductivity of the near-surface soil.

## ACKNOWLEDGMENTS

This project was supported by the National Research Initiative of the USDA Cooperative State Research, Education and Extension Service, grant number 2006-35107-17245 and by the University of Wisconsin Eau Claire.

## REFERENCES

- Grote, K., T. Crist, and C. Nickel (2010), Experimental estimation of the GPR groundwave sampling depth, Water Resour. Res., 46, W10520, doi:10.1029/2009WR008403.
- Topp, G.C., J.L. Davis, and A.P. Annan (1980), Electromagnetic determination of soil water content: measurements in coaxial transmission lines, Water Resour. Res., 16(3), 574-582.